2025 10th International Conference on Applying New Technology in Green Buildings (ATiGB)

Enhanced Semi-Active Suspension System for Electric Vehicles Utilising Combined Sky-Hook and Ground-Hook Control Strategies

1st Le Dinh Hieu
School of Engineering and Technology
Hue University, Vietnam
ledinhhieu@hueuni.edu.vn

***Abstract*—This research presents an improved semi-active suspension model derived from the conventional suspension system, incorporating a control strategy combining the Sky-hook and Ground-hook algorithms. To validate the effectiveness of this method, a state simulation was conducted to compare the improved suspension system with the conventional suspension system. The first test used an input chirp signal in the range of 0–20 Hz with an amplitude of 0.015 m. The second test involved a cosine speed bump signal with a duration of 2s and a height of 0.05 m. The final test simulated random road excitations using MATLAB-Simulink. The simulation results showed that the improved suspension system achieved 50.86 % faster vibration damping, improving the driving comfort and reducing the settling time by 55.14 %, improving the overall stability of the system.**

Keywords—semi-active suspension, vehicle suspension, sky-hook, ground-hook

I. Introduction

With advancements in science and technology, the demand for suspension systems in electric vehicles is increasing to enhance ride comfort and vehicle body stability [1, 2]. Currently, there are three main types of suspension systems: passive, semi-active, and active. This paper focuses on improving passive suspension into a semi-active system to achieve better damping force control [3-5].

A passive suspension system consists of a spring and a damper but lacks the ability to adjust damping force. In contrast, a semi-active suspension system can modulate damping force according to road conditions using technologies such as electrorheological (ER) and magnetorheological (MR) fluids [6, 7]. This study employs an ER fluid-based system combined with a control algorithm to optimize damping performance [8].

The control strategy utilizes the Sky-hook and Ground-hook algorithms to optimize ride comfort and stability. The Sky-hook algorithm acts as a virtual damper between the sprung mass and an inertial reference frame, reducing vibrations transmitted from the road to the vehicle, thereby improving passenger comfort [9-13]. The Ground-hook algorithm is linked to the unspring mass to minimize tire oscillations and enhance stability [14]. By combining both algorithms, the semi-active suspension system outperforms passive systems: Sky-hook prioritizes comfort, while Ground-hook focuses on stability. The damping force is calculated to simultaneously optimize both criteria [15, 16].

II. Ease of Use

This research proposes a semi-active suspension system and evaluates its stability through a state simulation process comparing two suspension systems. The first test uses a chirp signal as the input, ranging from 0-20 Hz with exhibiting an amplitude of 0.015m. The second test involves a cosine-shaped speed bump with a crossing time of 2sec and a height of 0.05m. The final test applies to a random excitation signal simulating an uneven road surface. These tests enable a comparison between the two models and help determine the relative improvement in optimization criteria.

A. *The quarter-car suspension model and its mathematical model.*

The improved suspension system model incorporates a dynamic damper with mass m_3, spring stiffness k_3, damping coefficient b_3, which reduces the excitation $z_1 - z_0$, z_2, and $\ddot{z}_2$, thereby increasing comfort and stability. Additionally, the active damper, which can control the actual damping F_b, is added and controlled using the Sky-hook and Ground-hook algorithms.

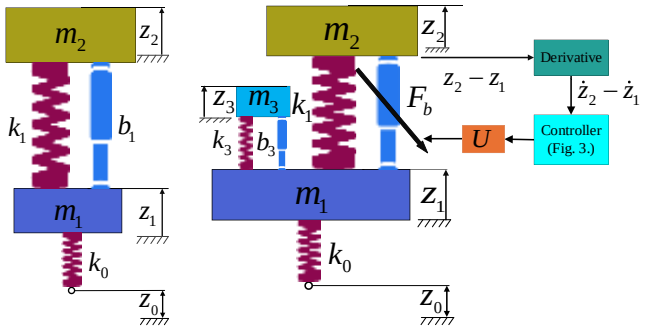

a) b)

Fig. 1. Quarter-car suspension model: a) Traditional; b) Improved with dynamic damper and semi-active shock absorber.

TABLE I. The Parameters Of The Suspension Components Used

Parameter	Symbol	Unit	Value
Unspring mass	m_1	Kg	55
Sprung mass	m_3	Kg	590,7
Extended absorber mass	m_3	Kg	30
Tire stiffness	k_o	N/m	202000
Spring stiffness	k_1	N/m	78100

Parameter	Symbol	Unit	Value
Damper stiffness	b_1	N.s/m	2369,6
Damping coefficient of the extended absorber	b_3	N.s/m	555
Natural frequency of the system	f_1	Hz	12
Sky-hook damper stiffness	b_s	N.s/m	6000
Ground-hook damper stiffness	b_g	N.s/m	-2300

B. Mathematical model of a traditional suspension system.

The dynamic equation of the traditional suspension system

$$\ddot{z}_2 = -\left(\frac{k_1}{m_2}\right)(z_2 - z_1) - \left(\frac{b_1}{m_2}\right)(\dot{z}_2 - \dot{z}_1) \quad (1)$$

$$\ddot{z}_1 = \left(\frac{k_1}{m_1}\right)(z_2 - z_1) + \frac{b_1}{m_1}(\dot{z}_2 - \dot{z}_1) - \left(\frac{k_0}{m_1}\right)(z_1 - z_0) \quad (2)$$

The differential equations will be transformed into state-space form with the expression of $x = Ax + Bu$, $y = Cx + Du$ and the variables $z_1 - z_0$, z_2 and $\ddot{z}_2$.

$$\begin{bmatrix}\dot{z}_2\\ \dot{z}_2\\ \dot{z}_1\\ \dot{z}_1\end{bmatrix} = \begin{bmatrix} 0 & 1 & 0 & 0 \\ -\frac{k_1}{m_2} & -\frac{b_1}{m_2} & \frac{k_1}{m_2} & \frac{b_1}{m_2} \\ 0 & 0 & 0 & 1 \\ \frac{k}{m_1} & \frac{b_1}{m_1} & -\frac{k_1}{m_1}-\frac{k_0}{m_1} & -\frac{b_1}{m_1} \end{bmatrix} \begin{bmatrix} z_2\\ \dot{z}_2\\ z_1\\ \dot{z}_1\end{bmatrix} + \begin{bmatrix} 0\\ 0\\ 0\\ \frac{k_{01}}{m_1}\end{bmatrix} z_0 \quad (3)$$

$$\begin{bmatrix}\ddot{z}_2\\ z_2\\ z_1 - z_0\end{bmatrix} = \begin{bmatrix} -\frac{k_1}{m_2} & -\frac{b_1}{m_2} & \frac{k_1}{m_2} & \frac{b_1}{m_2} \\ 1 & 0 & 0 & 0 \\ 0 & 0 & 1 & 0 \end{bmatrix} \begin{bmatrix} z_2\\ \dot{z}_2\\ z_1\\ \dot{z}_1\end{bmatrix} + \begin{bmatrix} 0\\ 0\\ -1\end{bmatrix} z_0 \quad (4)$$

Optimization functions for comfort and stability:

$$J_p = \int_{f_{\min}}^{f_{\max}} |G_p|^2 df = \int_{0Hz}^{20Hz} \left|\frac{\ddot{z}_2(f)}{z_0(f)}\right|^2 df \quad (5)$$

$$J_s = \int_{f_{\min}}^{f_{\max}} |G_s|^2 df = \int_{0Hz}^{20Hz} \left|\frac{z_1(f) - z_0(f)}{z_0(f)}\right|^2 df \quad (6)$$

Where:

Conveying comfort: $G_p = \frac{\ddot{z}_2}{z_0}$ (7)

Conveying stability: $G_s = \frac{z_1 - z_0}{z_0}$ (8)

C. Mathematical model of the improved suspension system.

The dynamic shock absorber and semi-active shock absorber suspension system model, the differential equation describing the motion will be as follows:

$$m_2\ddot{z}_2 = -k_1(z_2 - z_1) - b_1(\dot{z}_2 - \dot{z}_1) \quad (9)$$

$$\begin{aligned} m_1\ddot{z}_1 &= k_1(z_2 - z_1) + b_1(\dot{z}_2 - \dot{z}_1) + k_3(z_3 - z_1) \\ &+ b_3(\dot{z}_3 - \dot{z}_1) - F_1 - k_0(z_1 - z_0) \end{aligned} \quad (10)$$

$$m_3\ddot{z}_3 = -k_3(z_3 - z_1) - b_3(\dot{z}_3 - \dot{z}_1) + F_b \quad (11)$$

State-space matrix transformation:

$$\dot{\vec{x}} = \underline{A}\vec{x} + \underline{B}\vec{u},\ \vec{y} = \underline{C}\vec{x} + \underline{D}\vec{u},\ u = \begin{bmatrix} z_0 & \dot{z}_0 & F_b \end{bmatrix}^{\mathrm{T}}$$

$$\vec{x} = \begin{bmatrix} z_2 & \dot{z}_2 & z_1 - z_0 & \dot{z}_1 & z_3 & \dot{z}_3 \end{bmatrix}^{\mathrm{T}},\ \vec{y} = \begin{bmatrix} \ddot{z}_2 & z_2 & z_1 - z_0 \end{bmatrix}^{\mathrm{T}} \quad (12)$$

$$\underline{A} = \begin{bmatrix} 0 & 1 & 0 & 0 & 0 & 0 \\ -\frac{k_1}{m_2} & -\frac{b_1}{m_2} & \frac{k_1}{m_2} & \frac{b_1}{m_2} & 0 & 0 \\ 0 & 0 & 0 & 1 & 0 & 0 \\ \frac{k_1}{m_1} & \frac{b_1}{m_1} & -\frac{k_1}{m_1}-\frac{k_3}{m_1}-\frac{k_{01}}{m_1} & -\frac{b_1}{m_1}-\frac{b_3}{m_1} & \frac{k_3}{m_1} & \frac{b_3}{m_1} \\ 0 & 0 & 0 & 0 & 0 & 1 \\ 0 & 0 & \frac{k_3}{m_3} & \frac{b_3}{m_3} & -\frac{k_3}{m_3} & -\frac{b_3}{m_3} \end{bmatrix} \quad (13)$$

$$\underline{B} = \begin{bmatrix} \underline{B_D}, \underline{B_{Dd}}, \underline{B_c} \end{bmatrix},\ \underline{B_D} = \begin{bmatrix} 0 & \frac{k_1}{m_2} & 0 & -\frac{k_1}{m_1}-\frac{k_3}{m_1} & 0 & \frac{k_3}{m_3} \end{bmatrix}^{\mathrm{T}}$$

$$\underline{B_c} = \begin{bmatrix} 0 & 0 & 0 & -\frac{1}{m_1} & 0 & \frac{1}{m_3} \end{bmatrix}^{\mathrm{T}} \quad (14)$$

$$\underline{C} = \begin{bmatrix} -\frac{k_1}{m_2} & -\frac{b_1}{m_2} & \frac{k_1}{m_2} & \frac{b_1}{m_2} & 0 & 0 \\ 1 & 0 & 0 & 0 & 0 & 0 \\ 0 & 0 & 1 & 0 & 0 & 0 \end{bmatrix},\ \underline{D} = \begin{bmatrix} \frac{k_1}{m_2} & 0 & 0 \\ 0 & 0 & 0 \\ 0 & 0 & 0 \end{bmatrix} \quad (15)$$

D. Mathematical model of the improved suspension system.

This characteristic is chosen so that its lower limit corresponds to one third of the initial stiffness of the damping component and its upper limit corresponds to three times the initial stiffness. It is calculated using formulas (16) - (17) and is illustrated in Fig. 3.

Maximum damping force $F_{\max}$: $F_{\max} = 3b_1$ (16)

Minimum damping force $F_{\min}$: $F_{\min} = b_1 \cdot 3^{-1}$ (17)

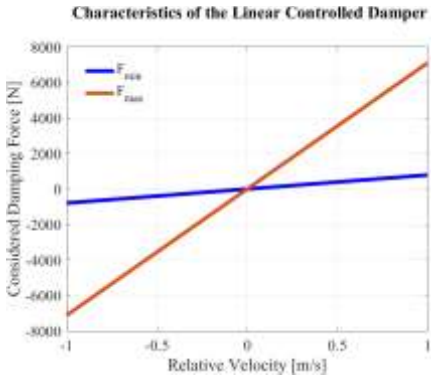

Fig. 2. The maximum and minimum damping coefficients.

To control the system, we convert and use the formula for calculating the required control voltage U based on the

required damping force F_a and the relative velocity v_{rel}, as given by the equation (19) below.

$$v_{rel} = z_2 - z_1 \tag{18}$$

The required damping force.

$$F_a = F_{b,s} + F_{b,g} = b_s \cdot \dot{z}_2 + b_g \cdot (\dot{z}_1 - \dot{z}_0) \tag{19}$$

$$U_{rid} = U_{max} - \frac{(F_{max}(v_{rel}) - F_a)(U_{max} - U_{min})}{F_{max}(v_{rel}) - F_{min}(v_{rel})} \tag{20}$$

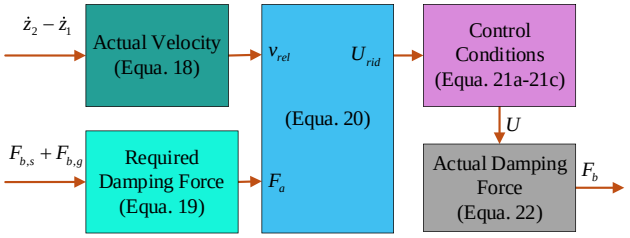

Fig. 3. Control system.

$$\text{If } U_{rid} > U_{max} \Rightarrow U = U_{max} \tag{21.a}$$

$$\text{If } U_{max} > U_{rid} > U_{min} \Rightarrow U = U_{rid} \tag{21.b}$$

$$\text{If } U_{rid} < U_{min} \Rightarrow U = U_{min} \tag{21.c}$$

The actual damping force F_b :

$$F_b = F_{max}(v_{rel}) + \frac{(U - U_{max})(F_{max}(v_{rel}) - F_{min}(v_{rel}))}{U_{max} - U_{min}} \tag{22}$$

The magnitude of the virtual damping force.

$$F_{b,s} = b_s \cdot \dot{z}_2 \tag{23}$$

$$F_{b,g} = b_g \cdot (\dot{z}_1 - \dot{z}_0) \tag{24}$$

Optimization function for comfort: $J_{pt} = \int_0^T \ddot{z}_2^2 \, dt$ (25)

And for stability: $J_{st} = \int_0^T (z_1 - z_0)^2 \, dt$ (26)

III. Results and Discussion

In this section, the paper will introduce the road surface type and speed bump types used for the experimental survey as follows: speed bump type 0.015 m (rumble strip type) and 0.05 m (speed bump type) (based on QCVN 41:2019/BGTVT, UK Traffic Advisory Leaflet 7/96) on asphalt concrete road type (TCVN 8867:2011, EU-EN 12697 with British Pendulum number > 60). This road surface type and speed bump types are applied to warn when the vehicle enters residential areas, schools, or highways.

The simulation results are obtained from the mathematical equations (1)-(26) and integrated with the modeling in Matlab-Simulink software to highlight and emphasize the results presented in Fig. 4 to Fig. 6.

The first test uses a Chirp type excitation signal in the frequency range 0–20 Hz. This frequency range corresponds approximately to the frequency at which the vehicle is excited by road irregularities during operation. Therefore, it will be possible to observe the system response on all frequencies in the selected frequency range for 100 s as depicted in Fig. 1. In general, semi-active suspension systems have better damping performance than conventional suspension systems. The comparisons are shown in Table 2 shows that during the initial period 0 -38 s, the improved semi-active suspension system demonstrates superior comfort.

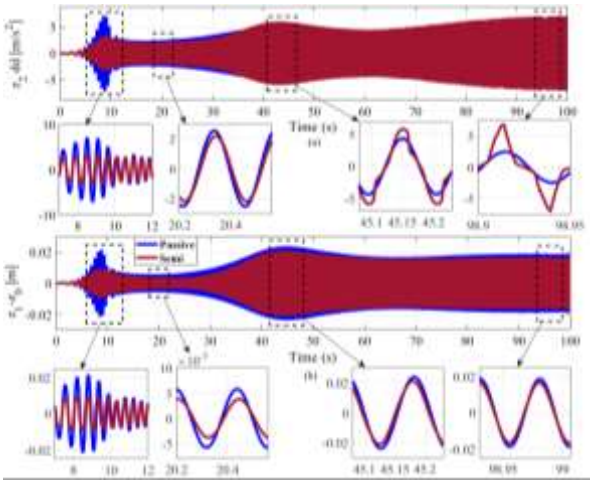

Fig. 4. Exciting the two suspension systems with a Chirp signal in the range of 0–20Hz with a magnitude of 0.015 m: (a) $\ddot{z}_2$, (b) $z_1 - z_0$

TABLE II. Comparison Of Two Bamboo Systems Through First Test

Parameters	Unit	Time (s)				ADR
		8.78 s	20.32 s	45.14 s	98.91 s	
Passive $\ddot{z}_2$	m/s2	7.23	2.51	4.36	2.39	
Semi $\ddot{z}_2$	m/s2	3.30	2.10	5.80	6.76	
Difference ratio $\ddot{z}_2$	%	54.4	16.3	- 33	-182	-36
Passive $z_1 - z_0$	m	0.022	0.005	0.024	0.019	
Semi $z_1 - z_0$	m	0.009	0.003	0.020	0.016	
Difference ratio $z_1 - z_0$	%	59.1	40.0	16.7	15.8	32

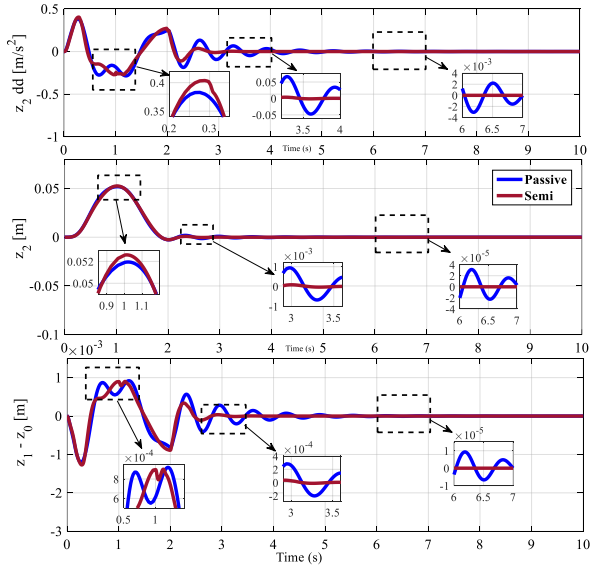

Fig. 5. Excitation with a signal for the system to pass over a cosine-shaped speed bump with a duration of 2s and a height of 0.05 m.

However, from 38-100 s, comfort is compromised as the oscillation frequency increases, with an average comfort deviation of -36 %. In terms of stability, the semi-active suspension performs even better, maintaining full control despite increasing oscillation frequency, with an average stability deviation of 32 %.

Furthermore, when the second experiment was performed using the excitation signal passing over a cosine speed bump with a height of 0.05 m in 2 s. The simulation results showed significant improvements for all three parameters $\ddot{z}_2$, z_2 and $z_1 - z_0$. The comparison data will be specifically mentioned in Table 3 with smaller oscillation time and amplitude when undergoing the test.

TABLE III. PARAMETERS OF THE TWO SYSTEMS IN TERMS OF TIME AND AMPLITUDE

Parameters	*Unit*	Times (s)		
		Passive	*Semi*	*Difference ratio*
$\ddot{z}_2$	s	7 s	3.44 s	50.86 %
z_2	s	7 s	3.13 s	55.29 %
$z_1 - z_0$	s	7 s	3.14 s	55.14 %
		Amplitude		
		Passive	*Semi*	*Difference ratio*
$\ddot{z}_2$	m/s^2	0.277	0.245	11.55 %
z_2	m	0.0518	0.0525	-1.33 %
$z_1 - z_0$	m	0.0009	0.0008	11.11 %

Table 2 shows the difference between the two systems in terms of damping time and amplitude. The semi-active suspension system reduced the amplitude of oscillation but for parameter z_2 it had a larger amplitude of 1.33 %, but the remaining two parameters still showed superiority with $\ddot{z}_2$ being 11.55 % and $z_1 - z_0$ have 11.11 %. Furthermore, the semi-active suspension system did really well in damping oscillation better for all three parameters: $\ddot{z}_2$ was 50.86 %, z_2 was 55.29 % and finally $z_1 - z_0$ was 55.14 %. Because the oscillation of the passive suspension system is almost zero after 7-10 s, in this study, the stabilization time hook of this system was chosen to be 7.0 s…

When moving on the road, it is impossible not to mention a type of continuous and irregular oscillation. For example, the road is continuously uneven, ... Therefore, the final test in this experiment will simulate this type of road most realistically when using the input signal as a random excitation signal for 10 s. The comparison The data reveals that the semi-active suspension system has controlled the oscillation. but not well for the parameter Z_{2dd}. There is still an overshoot leading to the oscillation amplitude of this system being larger than the passive system.

TABLE IV. COMPARISON FOR RANDOM INPUT SIGNAL TEST

Parameters	Unit	Time (s)			ADR
		2 s	5.05 s	9.5 s	
Passive $\ddot{z}_2$	m/s2	1.57	1.07	1.57	
Semi $\ddot{z}_2$	m/s2	0.27	1.36	2.00	
Difference ratio $\ddot{z}_2$	%	82.80	-27.10	- 27.39	9.44
Passive z_2	m	1.97	0.016	0.024	
Semi z_2	m	0.11	0.026	0.020	
Difference ratio z_2	%	94.42	-62.50	16.67	16.2
Passive $z_1 - z_0$	m	0.005	0.001	0.006	
Semi $z_1 - z_0$	m	0.002	0.0015	0.005	
Difference ratio $z_1 - z_0$	%	60.00	-50.00	16.70	8.9

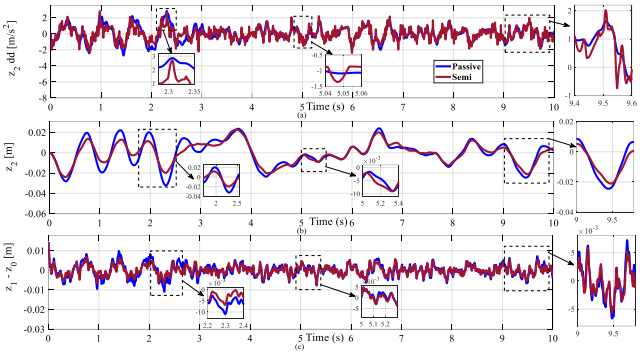

Fig. 6. The input signal is a random oscillation signal: (a) $\ddot{z}_2$,(b) z_2 , (c) $z_1 - z_0$

As seen in table 4 and overview in figure 6 semi-active suspension system controlled the oscillation in the range of 0-4 s and from 9.1 s for two parameters z_2 dd and z_1 - z_0. but better than that for parameter z_2 was controlled better than semi-active suspension system in the range of 0-10 s and achieved an average difference of 16.2 %

IV. CONCLUSION

The suspension system with a dynamic damper and semi-active shock absorber, using a combination of the Sky-hook and Ground-hook algorithms, is one of the highly effective solutions. Compared with typical suspension systems, this system has demonstrated significant advantages through the proposed tests. The results of this paper serve as a foundation for developing and optimizing the semi-active suspension system from the traditional suspension system model. Further development can be made by integrating a controller with other algorithms to achieve higher system performance. In particular, the combination with the LQR control algorithm can be applied.

REFERENCES

[1] H. Xu, J. Liu, T. Luo, Y. Yao, and C. Lv, "Model-Based Design of an Active Suspension for the Improvement of In-Wheel Motor Drive Electric Vehicle," *IEEE Access*, 2024.

[2] A. S. Gad, W. G. Ata, H. M. El-Zomor, and S. D. Jabeen, "Optimizing Driver Comfort: Magnetorheological Damper Seat Suspension for Internal Combustion and Electric Vehicles Under Uncertain Conditions," *Journal of Vibration Engineering & Technologies*, vol. 13, no. 2, p. 157, 2025.

[3] H. He, Y. Li, J. Z. Jiang, S. Burrow, S. Neild, and A. Conn, "Using an inerter to enhance an active-passive-combined vehicle suspension system," *International Journal of Mechanical Sciences*, vol. 204, p. 106535, 2021.

[4] A. Qin, B. Zhang, D. Ning, B. Tan, and H. Du, "A self-sensing approach for estimating suspension displacement and velocity in semi-active electromagnetic dampers," *Mechanical Systems and Signal Processing*, vol. 208, p. 111049, 2024.

[5] X. Shi, Q. Yu, Z. Wu, J.-Y. Li, and S. Zhu, "Active control for vehicle suspension using a self-powered dual-function active electromagnetic damper," *Journal of Sound and Vibration*, vol. 569, p. 117976, 2024.

[6] X. Tang, D. Ning, H. Du, W. Li, and W. Wen, "Takagi-Sugeno fuzzy model-based semi-active control for the seat suspension with an electrorheological damper," *IEEE Access*, vol. 8, pp. 98027-98037, 2020.

[7] M. Kumbhar, R. Desavale, and T. Jagadeesha, "Experimentation and damping performance analysis of a MR damper for resonance control in a quarter car suspension system," *Journal of Vibration Engineering & Technologies*, vol. 12, no. 4, pp. 5973-5983, 2024.

[8] S. Liu *et al.*, "Enhancing the performance of electrorheological fluids by structure design," *Journal of Colloid and Interface Science*, vol. 675, pp. 1052-1058, 2024.

[9] C. Liu, L. Chen, H. P. Lee, Y. Yang, and X. Zhang, "Generalized skyhook-groundhook hybrid strategy and control on vehicle suspension," *IEEE Transactions on Vehicular Technology*, vol. 72, no. 2, pp. 1689-1700, 2022.

[10] H. Li *et al.*, "Optimization of Suspension Damping in High-Temperature Superconducting Maglev Based on Combined Skyhook-Groundhook Control," *IEEE Transactions on Applied Superconductivity*, 2024.

[11] Z. Li, W. Sun, and H. Gao, "Road-holding-oriented control and analysis of semi-active suspension systems," *Journal of Dynamic Systems, Measurement, and Control*, vol. 141, no. 10, p. 101010, 2019.

[12] D. Zhang, Z.-Y. Tao, K. Zhou, F.-R. Zhou, Q.-Y. Peng, and Y.-Y. Tang, "Improving the energy efficiency and riding comfort of high-speed trains across slopes by the optimized suspension control," *Energy*, vol. 307, p. 132660, 2024.

[13] M. F. Aladdin and J. Singh, "Modelling and simulation of semi-active suspension system for passenger vehicle," *Journal of Engineering Science and Technology*, vol. 7, pp. 104-107, 2018.

[14] Y. Li, X. Yang, Y. Shen, Y. Liu, and W. Wang, "Optimal design and dynamic control of the HMDV inertial suspension based on the ground-hook positive real network," *Advances in Engineering Software*, vol. 171, p. 103171, 2022.

[15] H. Pu *et al.*, "Design, analysis and testing of an inerter-based passive sky-hook damper," *International Journal of Mechanical Sciences*, vol. 260, p. 108633, 2023.

[16] S. Kopylov, Z. Chen, and M. A. Abdelkareem, "Acceleration based ground-hook control of an electromagnetic regenerative tuned mass damper for automotive application," *Alexandria Engineering Journal*, vol. 59, no. 6, pp. 4933-4946, 2020.